Hadley Centre Technical Note 96
Disaggregation of daily data in JULES

July 23, 2014

Karina Williams, Met Office, and Douglas Clark, Centre for Ecology and Hydrology

1 Introduction

The Joint UK Land Environment System (JULES) [Best et al., 2011, Clark et al., 2011] is a community land surface model that can be used both online as part of the Met Office Unified Modelling system and offline for impacts studies. It has been designed to run at short time scales, in order to exchange heat, momentum and moisture fluxes with an atmospheric model at model timesteps.

When run in offline mode, the meteorological data used to drive JULES is read from input files. This forcing data is often only available at a temporal resolution of three hours or coarser, due to the practical considerations in storing such a large amount of atmospheric model data and the difficulties of obtaining observational data at this resolution. JULES has been shown to be sensitive to the temporal resolution of the forcing data (e.g. Compton and Best [2011]).

In some cases, particularly for projects involving model intercomparisons (e.g. the Inter-Sectoral Impact Model Inter- comparison Project (ISI-MIP) [Warszawski et al., 2013] and EUPORIAS [Hewitt et al., 2013]), forcing data is only available at daily resolution. The absence of a diurnal cycle for temperature and radiation and any sort of sub-daily structure for precipitation makes this data completely unsuitable for forcing JULES directly. It is therefore necessary to perform some sort of data disaggregation. To date, two main approaches have been used to disaggregate daily data into sub-daily data for JULES: the WATCH [Weedon et al., 2011] approach, developed as part of the EU-funded Water and Global Change programme, and the IMOGEN approach, used in the IMOGEN modelling system [Huntingford et al., 2010] and the JULES runs for the ISI-MIP project [Davie et al., 2013, Dankers et al., 2013]. The WATCH project published standalone fortran routines to perform the disaggregation, whereas, in IMOGEN, the disaggregation is performed internally, as the IMOGEN configuration of JULES is running. These approaches differ significantly in their treatment of precipitation, with the WATCH disaggregator using a multiplicative cascade model to distribute the precipitation and the IMOGEN approach modelling the day's precipitation as arising from one event of constant intensity and globally specified duration.

In JULES 4.0, the IMOGEN approach to disaggregation is made available in the JULES trunk for standard (i.e. non-IMOGEN) runs. This report documents the method used and illustrates the dependence on the value of the convective rain duration parameter chosen by the user, using a development branch based on adding the disaggregation code to a branch of JULES 3.4.1, which has been merged with the JULES trunk.

2 Disaggregation method

In JULES 4.0, disaggregation of daily forcing data to JULES model timesteps (typically of the order of 30 minutes) can be switched on using the `l_daily_disagg` flag (see the JULES 4.0 manual for more details of the user interface). When this flag is set to `True`, the daily forcing data is disaggregated to model timesteps, which involves imposing a diurnal cycle on temperature and radiation and allocating the precipitation to a continuous series of model timesteps within the day. The pressure P and wind values are unchanged by the disaggregation code and the specific humidity is kept below the specific humidity at saturation. Any interpolation (specified by `interp` in `JULES_DRIVE`) is performed within JULES before the disaggregation code is called. The disaggregation of each variable is described in more detail in the following sections. The forcing variables required when `l_daily_disagg=T` are the same as those needed when `l_daily_disagg=F`, plus the temperature range for each grid box for each day.

2.1 Temperature

A diurnal cycle is imposed on the near-surface air temperature using the relation

$$T = T_0 + \frac{\Delta T}{2} \cos(2\pi \left(t - t_{T_{max}}\right) / t_{day}), \tag{1}$$

where T_0 and ΔT are the temperature and diurnal temperature ranges before disaggregation respectively. t_{day} is the length of a day. $t_{T_{max}}$ is the time of day where the temperature is highest and is calculated with the IMOGEN routine `sunny`, which assumes that $t_{T_{max}}$ occurs 0.15 of a daylength after local noon i.e.

$$t_{T_{max}} = \frac{t_{up} + t_{down}}{2} + 0.15 \left(t_{up} - t_{down}\right) \tag{2}$$

where t_{up} and t_{down} are sunrise and sunset times.

2.2 Specific humidity

The disaggregator code also ensures that the specific humidity q does not go above the specific humidity at saturation $q_{sat}(T, P)$, as calculated by the subroutine `qsat` i.e.

$$q = \min(q, q_{sat}(T, P)). \tag{3}$$

Note that this condition does not conserve water [1].

2.3 Radiation

The diurnal cycle imposed on the downward longwave radiation is a function of temperature, as in Huntingford et al. [2010], derived assuming black body radiation and that the diurnal cycle of temperature is a small perturbation,

$$R_{lw}^{down} = R_{lw,0}^{down} \left(4\frac{T}{T_0} - 3\right), \tag{4}$$

[1] After the model runs for this report were carried out, an extra option was added which keeps the relative humidity constant - see the manual for more information.

where $R_{lw,0}^{down}$ is the downward longwave radiation before disaggregation and R_{lw}^{down} is the downward longwave radiation after disaggregation.

The downward shortwave radiation is found by

$$R_{sw}^{down} = R_{sw}^{0,down} R_{norm}^{\odot} \quad (5)$$

where $R_{norm}^{\odot}$ is the solar radiation normalisation factor, calculated by the IMOGEN routine `sunny`, using the position of the sun in the sky at each timestep for each gridbox. $R_{sw,0}^{down}$ and R_{sw}^{down} are the downward shortwave radiation before and after disaggregation, respectively.

In a general run of JULES, the diffuse radiation can be given explicitly in the forcing data (this is not the case for IMOGEN runs). A diurnal cycle is imposed on this diffuse radiation using

$$R_{diff} = R_{diff}^{0} R_{norm}^{\odot} \quad (6)$$

2.4 Precipitation

The IMOGEN method of disaggregating the precipitation has two components:

- The entire day's precipitation of each type is first restricted to one event, of duration τ_x for $x =$ convective rain, large-scale rain, convective snow and large-scale snow respectively (in seconds). The start of the precipitation event is distributed randomly throughout the time period between the beginning of the day (in UTC) and τ_x before the end of the day.
- If the rate of precipitation in a timestep exceeds a maximum precipitation rate (hardwired in as 350 mm/day), then the precipitation is redistributed using the IMOGEN routine `redis`, which moves the excess precipitation to dry timesteps immediately before or after the sequence of wet timesteps, thus lengthening the event beyond τ_x. This step was included in IMOGEN because it was found that very high precipitation rates caused numerical issues for the Met Office Surface Exchange Scheme (MOSES) Essery et al. [2001], which evolved into JULES (for more details, see code comment in `src/imogenday_calc.F90`).

The mean diurnal cycle produced by this method is not a constant. Since rain events are not allowed to begin in one day and finish in the subsequent day, the timesteps near the beginning and end of the day (as defined by the time used internally in JULES, not by local time) will be wet less often than timesteps in rest of the day. This is illustrated in Figure 1, which shows the mean diurnal cycle for 100,000 days of precipitation for a range of event durations.

There are four options for precipitation disaggregation in JULES 4.0, specified by the value of the `precip_disagg_method` flag:

1. a constant value of precipitation rate is used for the entire day
2. the IMOGEN method

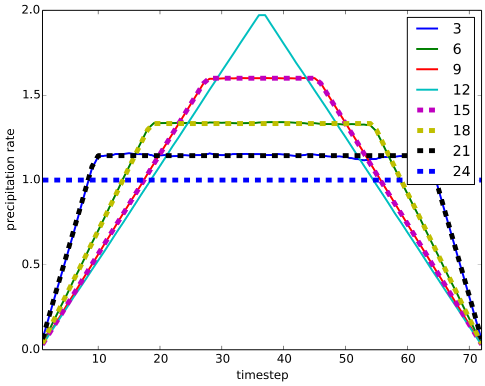

Figure 1: The diurnal cycle of simulated precipitation rate for 100,000 days, each with a mean daily precipitation rate normalised to one. The precipitation for each day has been disaggregated into 72 timesteps i.e the timestep length is 20 minutes. The legend shows the precipitation event duration in hours.

3. as for the IMOGEN method except precipitation does not get redistributed when the rate exceeds `max_precip_rate`

4. a proportion τ_x/t_{day} of the timesteps in the day are randomly selected to be wet, and the precipitation is distributed uniformly among them (t_{day} is the length of a day in seconds). This enforces a flat diurnal cycle of precipitation.

Global values of the precipitation event durations (τ_x) are set by the user (in `JULES_DRIVE`). The default values are $\tau_{conv\,rain} = 6 \times 3600\,\mathrm{seconds}$, $\tau_{ls\,rain} = \tau_{ls\,snow} = 1 \times 3600\,\mathrm{seconds}$. These have been taken from the defaults in IMOGEN at JULES 3.4.1. For ISI-MIP, $\tau_{conv\,rain} = 2 \times 3600\,\mathrm{seconds}$, $\tau_{ls\,rain} = \tau_{ls\,snow} = 5 \times 3600\,\mathrm{seconds}$, chosen to be physically reasonable. Convective snow was not given as input in IMOGEN or ISI-MIP. The duration of convective snow events has a default in JULES 4.0 of $\tau_{conv\,rain} = 1 \times 3600\,\mathrm{seconds}$.

3 Experimental setup

The performance of this disaggregation method was investigated using output from a global vn8.3 Met Office Unified Model (UM) run in the Global Atmosphere 4.0 (GA4.0) configuration [Walters et al., 2013] at a model timestep of 20 minutes as forcing data for an offline run of a branch of JULES 3.4.1 which had the disaggregation code added. This branch was merged with the JULES trunk before the release of JULES 4.0. The longwave radiation was pre-processed by copying the data value at the first timestep of each hour into the second and third timesteps of that hour, in order to eliminate errors that had been introduced by requiring model output at a higher resolution than the radiation timestep. The JULES namelists for the offline runs were based on the GL4.0 JULES configuration namelists, edited to be consistent with the UM run, including use of the same ancillary files.

The results from comparing an offline JULES run driven by this 20 minute forcing data was compared to the results when JULES was driven by daily means of this forcing data, which are disaggregated internally using `precip_disagg_method` = 3 (i.e. similar to IMOGEN method but with no maximum precipitation rate being enforced) and the diurnal temperature range and a range of convective rain event durations $\tau_{conv\,rain}$. For comparison, an additional run was done with three hourly driving data with interpolation (`interp` = 'f').

4 Results

4.1 Diurnal cycle

Fig 2 illustrates the mean diurnal cycle imposed by the disaggregator on the driving data, averaged over a year of the run (1984), as compared to the diurnal cycle of the model, using the Manaus FLUXNET site in Brazil as an example (see Appendix for a selection of other FLUXNET sites). As shown by Eq. 1 and Eq. 2, the disaggregator imposes a sinusoidal diurnal cycle on the temperature, which in general works reasonably well for the middle of the day but has a minimum earlier than the original 20 minute driving data; in the example of the Manaus site, this mimimum occurs four hours too early. The mean short wave diurnal profile is captured well by the disaggregator. However, the long wave diurnal profile of the original 20 minute forcing data has a much smaller amplitude than produced by the disaggregator using Eq. 4, and, as was the case for the temperature, the amount of time between the minimum and the following maximum in the original 20 minute driving data is less than would be expected if the diurnal cycle followed a sine curve. As stated in Section 1, no diurnal cycle is imposed on wind or pressure by the disaggregator. The specific humidity diurnal cycle is also not well matched by the disaggregator.

The convective rainfall produced by the disaggregator at the Manaus site is a good example of the limitations of the precipitation disaggregation method. Fig 2 shows disaggregated convective rainfall with a default event duration of 6 hours. In the original 20 minute driving data, there is a clear diurnal cycle. This is not reproduced at all in the disaggregated convective rainfall, which instead tends to roughly a trapezoidal pulse, with minimum at midnight UTC, as discussed in Section 2. Similarly, large-scale rainfall in the original 20 minute driving data has a diurnal cycle which is not well described by the disaggregator, using the default large-scale rain event duration value of one hour. If data from more years were included in this plot, the diurnal profile of the disaggregated large-scale rainfall between 01:00 UTC and 23:00 UTC would tend towards a flat line.

In addition to plotting the mean diurnal cycle, it would also be useful to investigate how well the variability is captured by the disaggregator. For example, short wave radiation would have variability introduced by sporadic cloud cover, which is not modelled by the disaggregator.

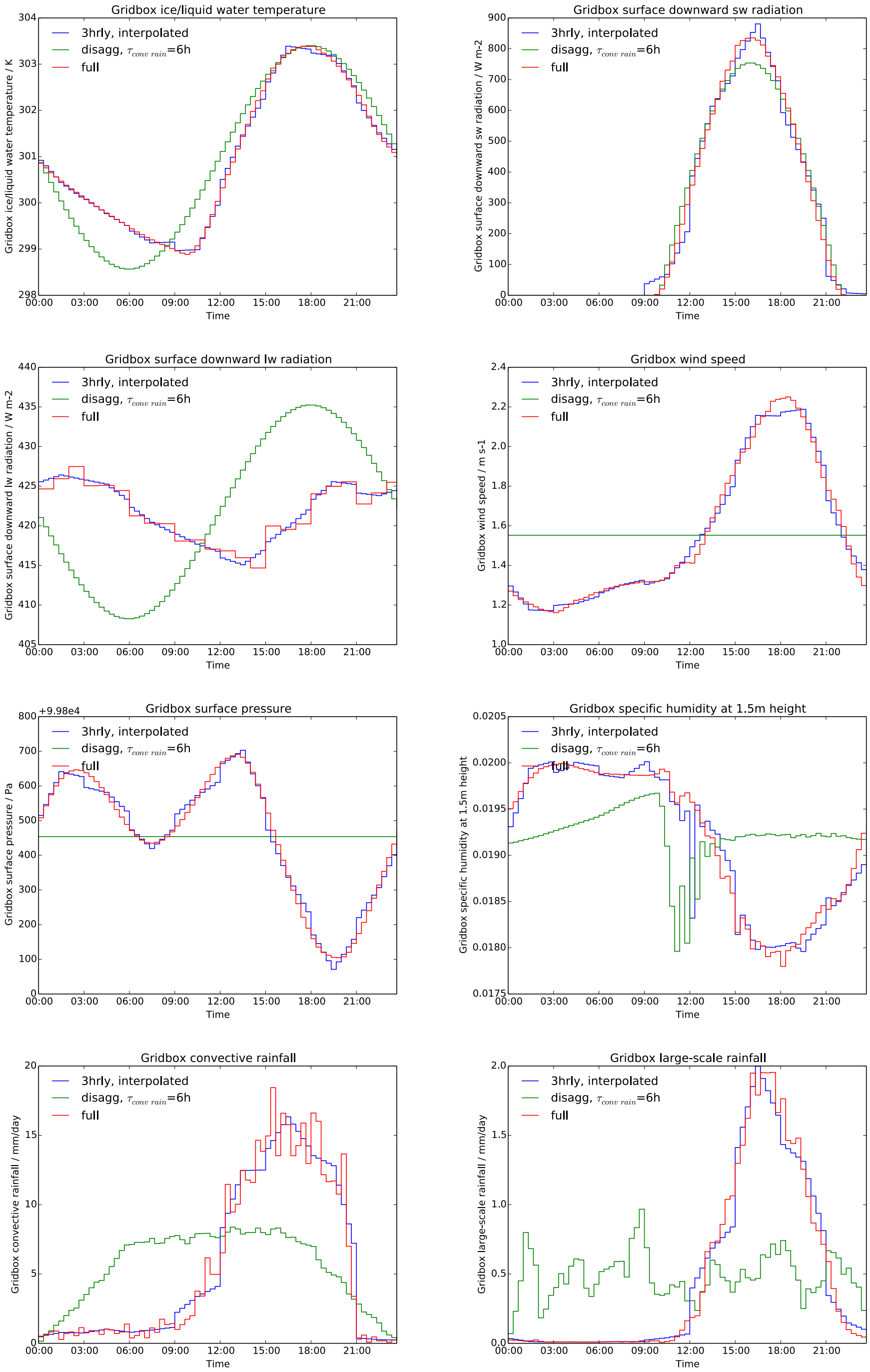

Figure 2: Diurnal cycle of driving data for the Manaus FLUXNET site, Brazil, averaged over the days in 1984.

4.2 Global climatology

Figure 3 (top left) shows the total evapotranspiration (total ET) over the full JULES offline run, which has forcing data at 20 minute resolution created by the UM run (described in Section 3). Figure 3 (bottom right) shows the anomaly from subtracting this result from a run forced with daily means and no disaggregation. Unsurprisingly, given the complete lack of diurnal cycle in this forcing data, these anomalies are very large, particularly in the tropics.

Figure 3 (bottom left) shows the anomaly in total evapotranspiration from a run forced with daily means and disaggregated internally in JULES to the model timestep with respect to the run driven by the full 20 minute UM output. The event durations have been kept at their default values. It can be seen that the use of the disaggregator reduces the anomalies drastically, implying that there is a significant advantage to using the disaggregator if only daily forcing data is available. However, this should be considered in the context of the anomalies from using 3 hourly forcing data with interpolation Figure 3 (top right), which are larger than the anomalies from using the disaggregator. Since 3 hourly forcing data with interpolation represents the model diurnal cycle and variability far better than this disaggregator can, this implies that the small anomalies in Figure 3 (bottom right) are perhaps due to a tuning of the disaggregator parameters to partially compensate for model biases.

There is also some compensation between the contribution of soil ET anomalies and canopy ET anomalies towards total ET, for example in South East Asia (Figure 7 and Figure 8 in the Appendix). The anomalies in the soil evapotranspiration in the equatorial regions are predominantly negative in the run driven by 3 hour means and daily means with no disaggregation, particularly in the tropics, and the anomalies in the soil evapotranspiration are predominantly positive.

Figure 4 shows the mean runoff in the full run (top left) and the anomalies with the respect to the full run for the 3 hourly-forced run (top right), the disaggregated run (bottom left) and the daily forced run without disaggregation (bottom right). Comparison with Figure 3 (bottom left) shows that the regions with large negative anomalies roughly coincide with the regions where the total evapotranspiration anomaly was high, as we would expect since the extra water added to the atmosphere through evaporation and transpiration is not available for inclusion in the runoff. Figure 4 also shows that the three hourly forced run and daily run have total runoff anomalies with a higher magnitude than the disaggregated run, also consistent with the total evapotranspiration results. In some areas, the contributions to the total runoff anomaly from surface runoff and sub-surface runoff act to compensate for eachother to a certain extent (Figure 9 and Figure 10 in the Appendix), such as in the region south and east of the Himalayas, where the disaggregated run shows a positive anomaly in the surface runoff and a negative anomaly in the sub-surface runoff.

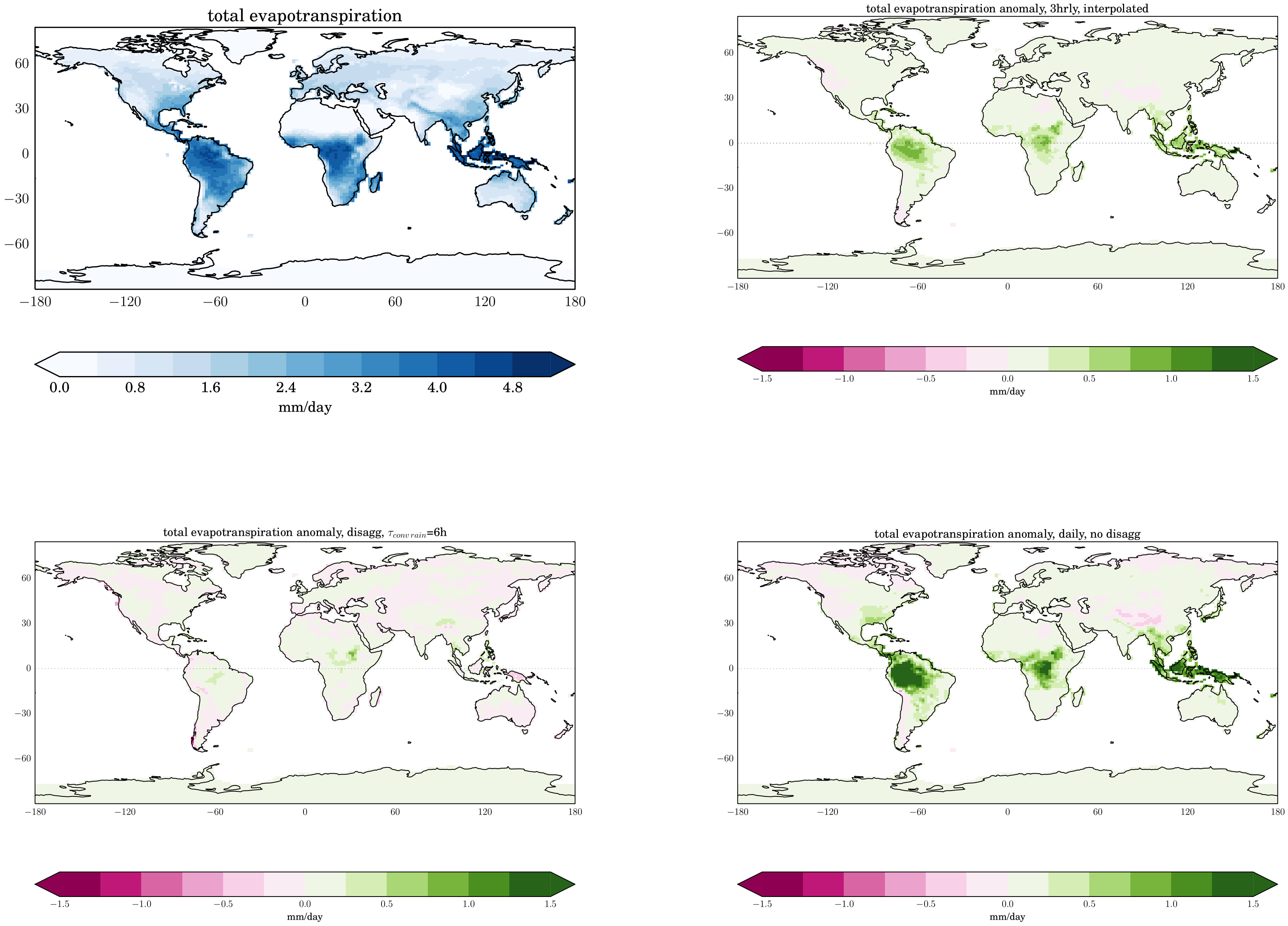

Figure 3: Top left: Output variable from JULES run with full 20 minute resolution forcing. Top right: Anomalies with respect to the full result, using 3 hourly forcing with interpolation. Bottom left: Anomalies with respect to the full result, using disaggregation with default event durations. Bottom right: Anomalies with respect to the full result, using daily forcing with no interpolation.

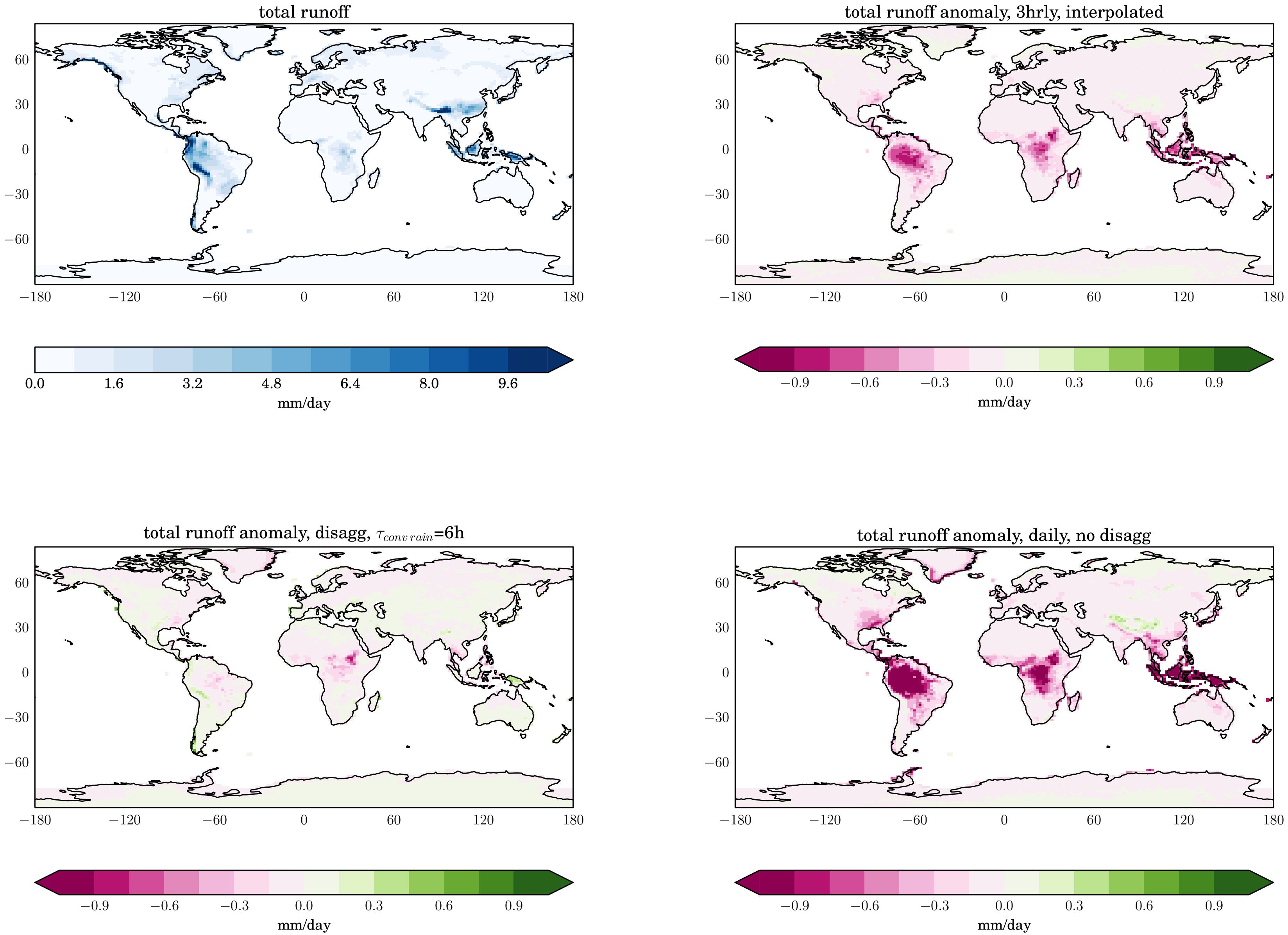

Figure 4: Top left: Output variable from JULES run with full 20 minute resolution forcing. Top right: Anomalies with respect to the full result, using 3 hourly forcing with interpolation. Bottom left: Anomalies with respect to the full result, using disaggregation with default event durations. Bottom right: Anomalies with respect to the full result, using daily forcing with no interpolation.

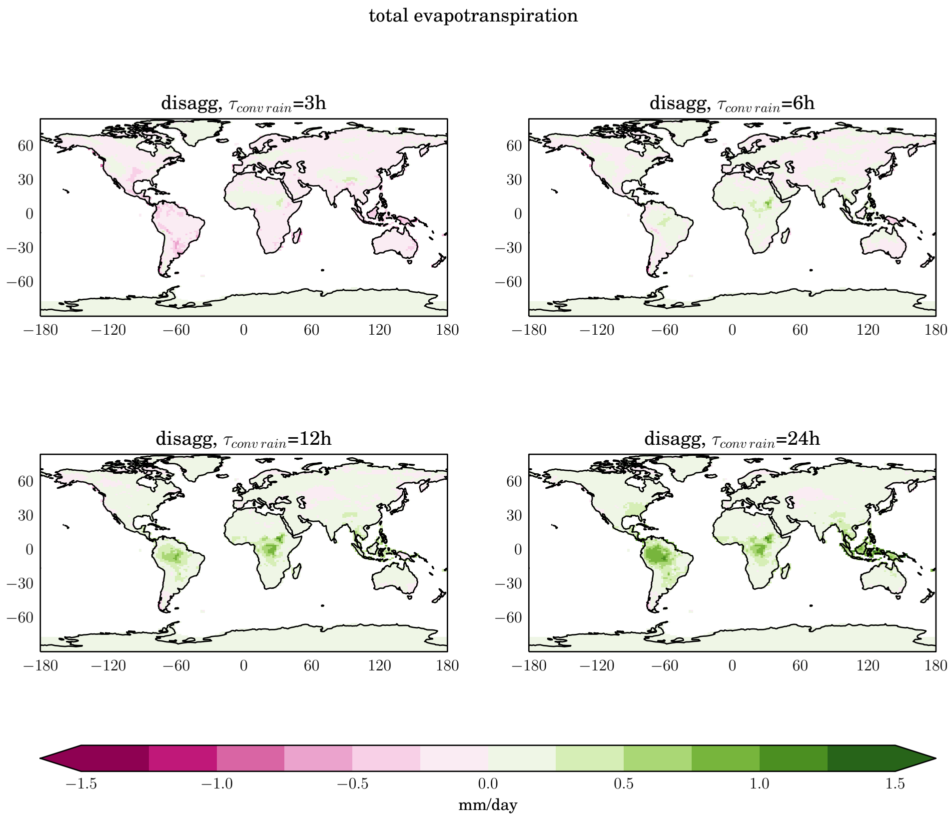

Figure 5: Anomalies with respect to the full result, using disaggregation with convective rain event durations of 3 hours (top left), 6 hours (top right), 12 hours (bottom left) and 24 hours (bottom right).

4.3 Dependence on the convective rain event duration

Figure 5 shows the anomalies of the disaggregated runs with respect to the full run for convective rain event duration parameters of $\tau_{conv\,rain}$ = 3h, 6h, 12h and 24h. Event duration parameters for the other types of precipitation are kept at their default values. The total evapotranspiration increases as $\tau_{conv\,rain}$ increases, as we would expect, as larger values of $\tau_{conv\,rain}$ means that the rainfall is less intense and lasts longer.

As the convective rain event duration increases, it is generally the case that soil ET decreases and canopy ET increases (Figure 11 and Figure 12 in the Appendix), as expected since the lower event durations give more intense rain, which penetrates the canopy better. In some regions, such as the Pampas in South America, which is predominantly modelled as C3 grass, soil evaporation increases as the convective rain event duration increases. For total ET, soil ET and canopy ET, using the disaggregator with the disaggregation of convective rainfall switched off (i.e. $\tau_{conv\,rain} = 24h$) is a significant improvement on using no disaggregation at all, illustrating the importance of the disaggregation of the other driving variables. Out of this selection of values for the convective rain event duration, $\tau_{conv\,rain} = 6h$ results in the lowest anomalies for total evapotranspiration, soil

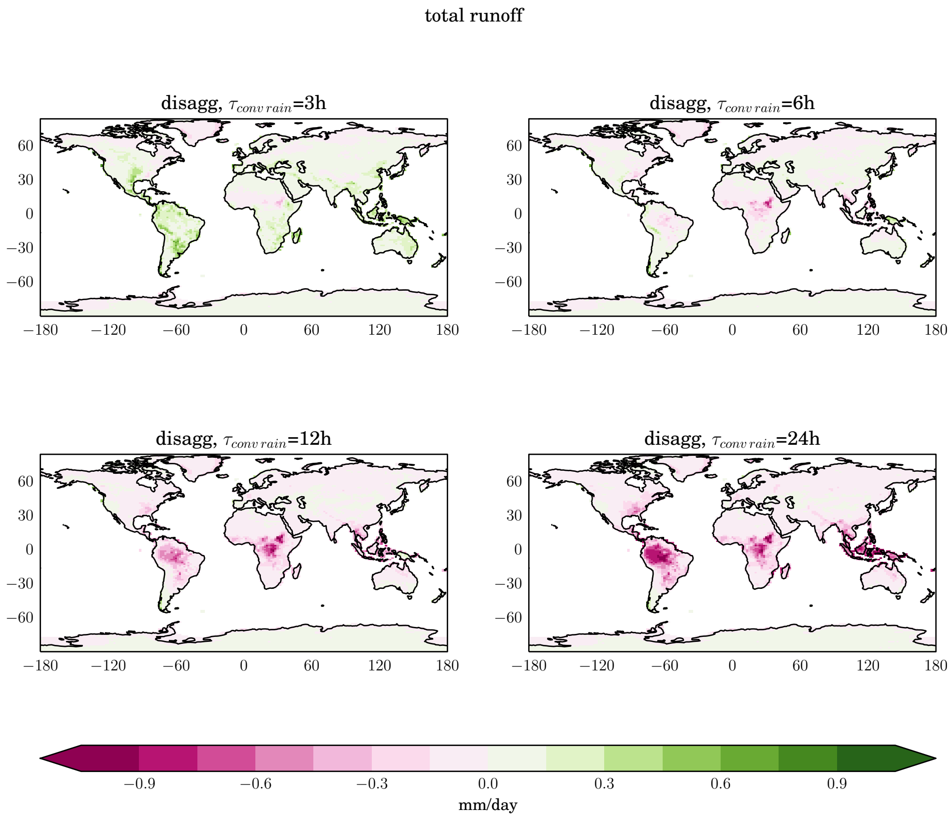

Figure 6: Anomalies with respect to the full result, using disaggregation with convective rain event durations of 3 hours (top left), 6 hours (top right), 12 hours (bottom left) and 24 hours (bottom right).

evapotranspiration and canopy evapotranspiration in general.

The runoff also depends strongly on the duration of the convective rain events, shown in Figure 6. As for evaporation, $\tau_{conv\,rain} = 6h$ appears to perform the best for total runoff out of the values of $\tau_{conv\,rain}$ illustrated here. As the duration decreases (and so the rainfall intensity increases), the surface runoff increases and sub-surface runoff decreases (Figure 13 and Figure 14 in the Appendix), as we would expect. In some regions, such as the Andes and the region south and east of the Himalayas for $\tau_{conv\,rain} = 3h$, the negative anomaly in sub-surface runoff roughly mirrors the positive surface runoff anomaly. In other regions, such as the Congo basin for $\tau_{conv\,rain} = 12h$, there is a large negative anomaly in surface runoff, but no correspondingly large anomaly in sub-surface runoff, leading to a large negative anomaly in the total runoff, consistent with the large positive anomaly in total evapotranspiration, which we saw in Figure 5 (top right).

In summary, in it generally the case that increasing the convective rain event duration parameter results in more of the rainfall being evaporated and less contributing to the runoff, particularly in equatorial regions. Evaporation and runoff are very sensitive to this parameter, which should be set with care. From the results shown here, using $\tau_{conv\,rain} = 6h$ appears to achieve a good compromise for most areas of the world. However, selecting the values of the event durations by tuning the evaporation and runoff anomalies could hide biases in the climatology of the model. There is good indication that this is happening here, since, as we saw in Section 4.2, using $\tau_{conv\,rain} = 6h$ can result in lower anomalies than using 3 hourly forcing data with interpolation.

5 Summary

A disaggregation option has been built in to JULES 4.0, which will allow offline runs to be forced by daily meteorological data, which is then disaggregated to the model timestep internally using the IMOGEN method. This option will be particularly useful for model intercomparisons, where subdaily forcing data is not always available. We describe the implementation of this method in detail and show an example of the resulting mean diurnal cycle of forcing variables after disaggregation.

We used UM output to force a set of offline JULES runs, to compare forcing at 20 minute resolution with forcing at three hourly resolution with interpolation and daily forcing with and without disaggregation. There was a clear advantage to using the disaggregator when using daily driving data. However, the disaggregated run with default parameters also reproduced the mean climate in some cases better than the 3-hourly forced run, which implies that these parameter values may be partially compensating for biases in the model. Since the results are sensitive to the disaggregation parameters, we would encourage the user to consider carefully which values are most appropriate for their individual needs and possibly to perform some initial analysis to assess the impact of this choice on the region, output variables and timescales they are most interested in.

An interesting next step would be to investigate the variability of the model output produced using the disaggregation option. It would also be useful to see how the disaggregator performs compared to high temporal resolution observational forcing data since, for example, there are known issues with the model diurnal cycle of precipitation [Stephens et al., 2010, Stratton and Stirling, 2012, Stirling and Stratton, 2012].

There are many ways in which this disaggregator could be improved, which we hope will be taken forward by the JULES community. For example, one simple extension would be to allow the precipitation event duration parameters to vary spatially, although the simplistic nature of the precipitation model (all the rainfall in one event, with constant intensity) means that it is not clear how the duration parameter could be derived from observed precipitation, even when these observations are available at sufficiently high temporal resolution. Other interesting possibilities would be to distribute the daily precipitation amongst the timesteps in that day using a cascade process, or allow the user to specify a normalised diurnal profile for each gridbox.

6 Acknowledgements

Many thanks to Pete Falloon, Martin Best and Andy Wiltshire for reading through various stages of the draft and their helpful advice and suggestions. We are also very grateful to Spencer Liddicoat, Camilla Mathison and James Manners for their assistance with the Unified Model set-up.

References

M. J. Best, M. Pryor, D. B. Clark, G. G. Rooney, Essery, C. B. Ménard, J. M. Edwards, M. A. Hendry, A. Porson, N. Gedney, L. M. Mercado, S. Sitch, E. Blyth, O. Boucher, P. M. Cox, C. S. B. Grimmond, and R. J. Harding. The Joint uk Land Environment Simulator (jules), model description Part 1: Energy and water fluxes. *Geoscientific Model Development*, 4(3):677–699, September 2011. doi: 10.5194/gmd-4-677-2011. URL `http://dx.doi.org/10.5194/gmd-4-677-2011`.

D. B. Clark, L. M. Mercado, S. Sitch, C. D. Jones, N. Gedney, M. J. Best, M. Pryor, G. G. Rooney, R. L. H. Essery, E. Blyth, O. Boucher, R. J. Harding, C. Huntingford, and P. M. Cox. The Joint uk Land Environment Simulator (jules), model description Part 2: Carbon fluxes and vegetation dynamics. *Geoscientific Model Development*, 4(3):701–722, September 2011. doi: 10.5194/gmd-4-701-2011. URL `http://dx.doi.org/10.5194/gmd-4-701-2011`.

Emma Compton and Martin Best. Impact of spatial and temporal resolution on modelled terrestrial hydrological cycle components. Technical Report 44, WATCH report, July 2011.

Rutger Dankers, Nigel W. Arnell, Douglas B. Clark, Pete D. Falloon, Balázs M. Fekete, Simon N. Gosling, Jens Heinke, Hyungjun Kim, Yoshimitsu Masaki, Yusuke Satoh, Tobias Stacke, Yoshihide Wada, and Dominik Wisser. First look at changes in flood hazard in the Inter-Sectoral impact model intercomparison project ensemble. *Proceedings of the National Academy of Sciences*, 111(9):201302078–3261, December 2013. ISSN 1091-6490. doi: 10.1073/pnas.1302078110. URL `http://dx.doi.org/10.1073/pnas.1302078110`.

J. C. S. Davie, P. D. Falloon, R. Kahana, R. Dankers, R. Betts, F. T. Portmann, D. B. Clark, A. Itoh, Y. Masaki, K. Nishina, B. Fekete, Z. Tessler, X. Liu, Q. Tang, S. Hagemann, T. Stacke, R. Pavlick, S. Schaphoff, S. N. Gosling, W. Franssen, and N. Arnell. Comparing projections of future changes in runoff and water resources from hydrological and ecosystem models in ISI-MIP. *Earth System Dynamics Discussions*, 4(1):279–315, February 2013. ISSN 2190-4995. doi: 10.5194/esdd-4-279-2013. URL http://dx.doi.org/10.5194/esdd-4-279-2013.

R. Essery, M. Best, and P. Cox. Moses 2.2 technical documentation. Technical Report 30, Hadley Centre, 2001. URL http://www.metoffice.gov.uk/media/pdf/9/j/HCTN_30.pdf.

Chris Hewitt, Carlo Buontempo, and Paula Newton. Using climate predictions to better serve society's needs. *Eos Trans. AGU*, 94(11):105–107, March 2013. doi: 10.1002/2013eo110002. URL http://dx.doi.org/10.1002/2013eo110002.

C. Huntingford, B. B. B. Booth, S. Sitch, N. Gedney, J. A. Lowe, S. K. Liddicoat, L. M. Mercado, M. J. Best, G. P. Weedon, R. A. Fisher, M. R. Lomas, P. Good, P. Zelazowski, A. C. Everitt, A. C. Spessa, and C. D. Jones. IMOGEN: an intermediate complexity model to evaluate terrestrial impacts of a changing climate. *Geoscientific Model Development*, 3(2):679–687, November 2010. doi: 10.5194/gmd-3-679-2010. URL http://dx.doi.org/10.5194/gmd-3-679-2010.

Graeme L. Stephens, Tristan L'Ecuyer, Richard Forbes, Andrew Gettlemen, Jean-Christophe Golaz, Alejandro Bodas-Salcedo, Kentaroh Suzuki, Philip Gabriel, and John Haynes. Dreary state of precipitation in global models. *J. Geophys. Res.*, 115(D24):D24211+, December 2010. ISSN 0148-0227. doi: 10.1029/2010jd014532. URL http://dx.doi.org/10.1029/2010jd014532.

A. J. Stirling and R. A. Stratton. Entrainment processes in the diurnal cycle of deep convection over land. *Q.J.R. Meteorol. Soc.*, 138(666):1135–1149, July 2012. doi: 10.1002/qj.1868. URL http://dx.doi.org/10.1002/qj.1868.

R. A. Stratton and A. J. Stirling. Improving the diurnal cycle of convection in GCMs. *Q.J.R. Meteorol. Soc.*, 138(666):1121–1134, July 2012. doi: 10.1002/qj.991. URL http://dx.doi.org/10.1002/qj.991.

D. N. Walters, K. D. Williams, I. A. Boutle, A. C. Bushell, J. M. Edwards, P. R. Field, A. P. Lock, C. J. Morcrette, R. A. Stratton, J. M. Wilkinson, M. R. Willett, N. Bellouin, A. Bodas-Salcedo, M. E. Brooks, D. Copsey, P. D. Earnshaw, S. C. Hardiman, C. M. Harris, R. C. Levine, C. MacLachlan, J. C. Manners, G. M. Martin, S. F. Milton, M. D. Palmer, M. J. Roberts, J. M. Rodríguez, W. J. Tennant, and P. L. Vidale. The Met Office Unified Model Global Atmosphere 4.0 and jules Global Land 4.0 configurations. *Geoscientific Model Development Discussions*, 6(2):2813–2881, May 2013. doi: 10.5194/gmdd-6-2813-2013. URL http://dx.doi.org/10.5194/gmdd-6-2813-2013.

Lila Warszawski, Katja Frieler, Veronika Huber, Franziska Piontek, Olivia Serdeczny, and Jacob Schewe. The Inter-Sectoral impact model intercomparison project (ISIMIP):

Project framework. *Proceedings of the National Academy of Sciences*, pages 201312330+, December 2013. ISSN 1091-6490. doi: 10.1073/pnas.1312330110. URL http://dx.doi.org/10.1073/pnas.1312330110.

G. P. Weedon, S. Gomes, P. Viterbo, W. J. Shuttleworth, E. Blyth, H. Österle, J. C. Adam, N. Bellouin, O. Boucher, and M. Best. Creation of the WATCH forcing data and its use to assess global and regional reference crop evaporation over land during the twentieth century. *J. Hydrometeor*, 12(5):823–848, March 2011. doi: 10.1175/2011jhm1369.1. URL http://dx.doi.org/10.1175/2011jhm1369.1.

A Additional plots: global climatology plots and diurnal cycles of forcing variables at FLUXNET sites

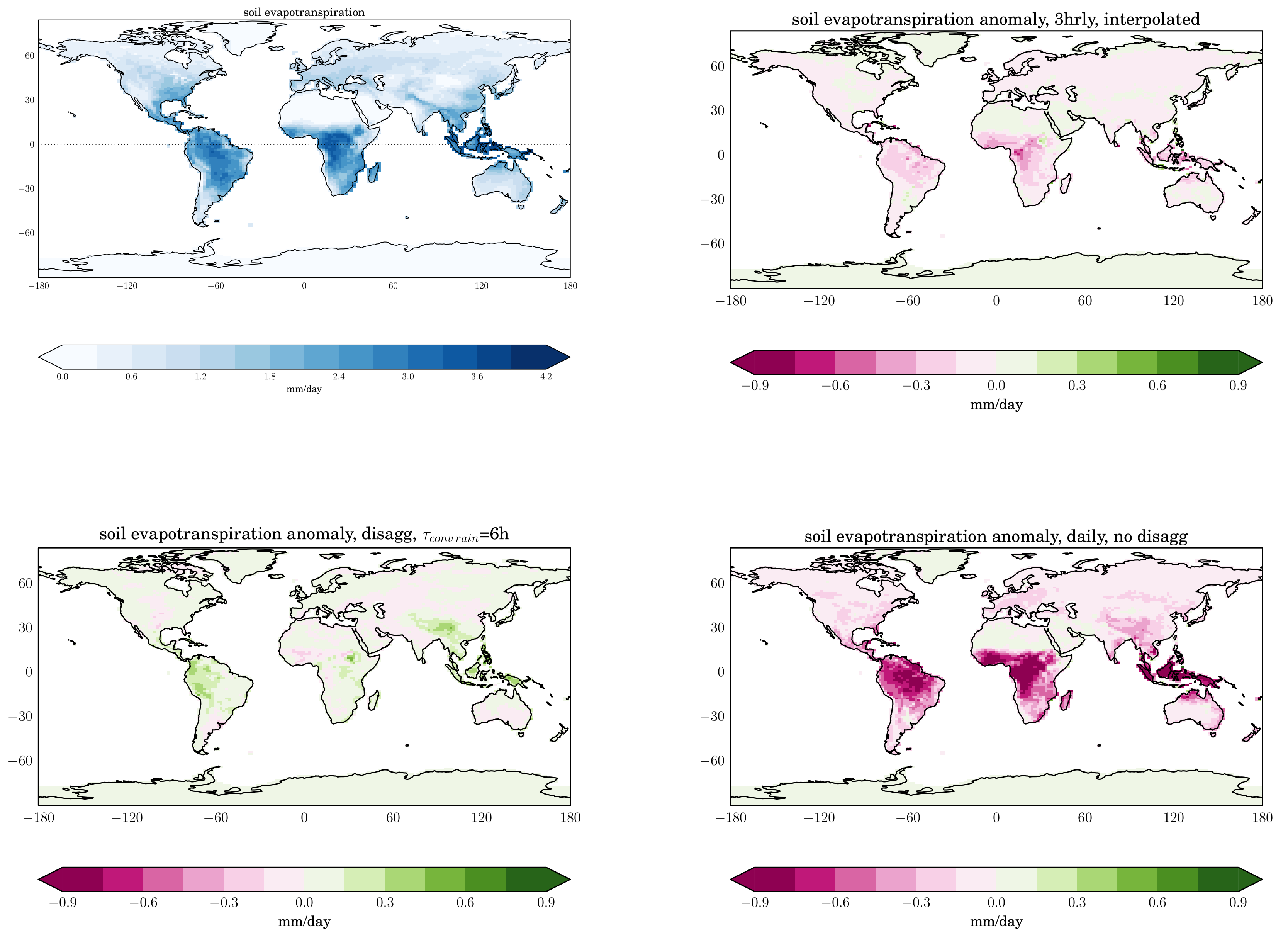

Figure 7: Top left: Output variable from JULES run with full 20 minute resolution forcing. Top right: Anomalies with respect to the full result, using 3 hourly forcing with interpolation. Bottom left: Anomalies with respect to the full result, using disaggregation with default event durations. Bottom right: Anomalies with respect to the full result, using daily forcing with no interpolation.

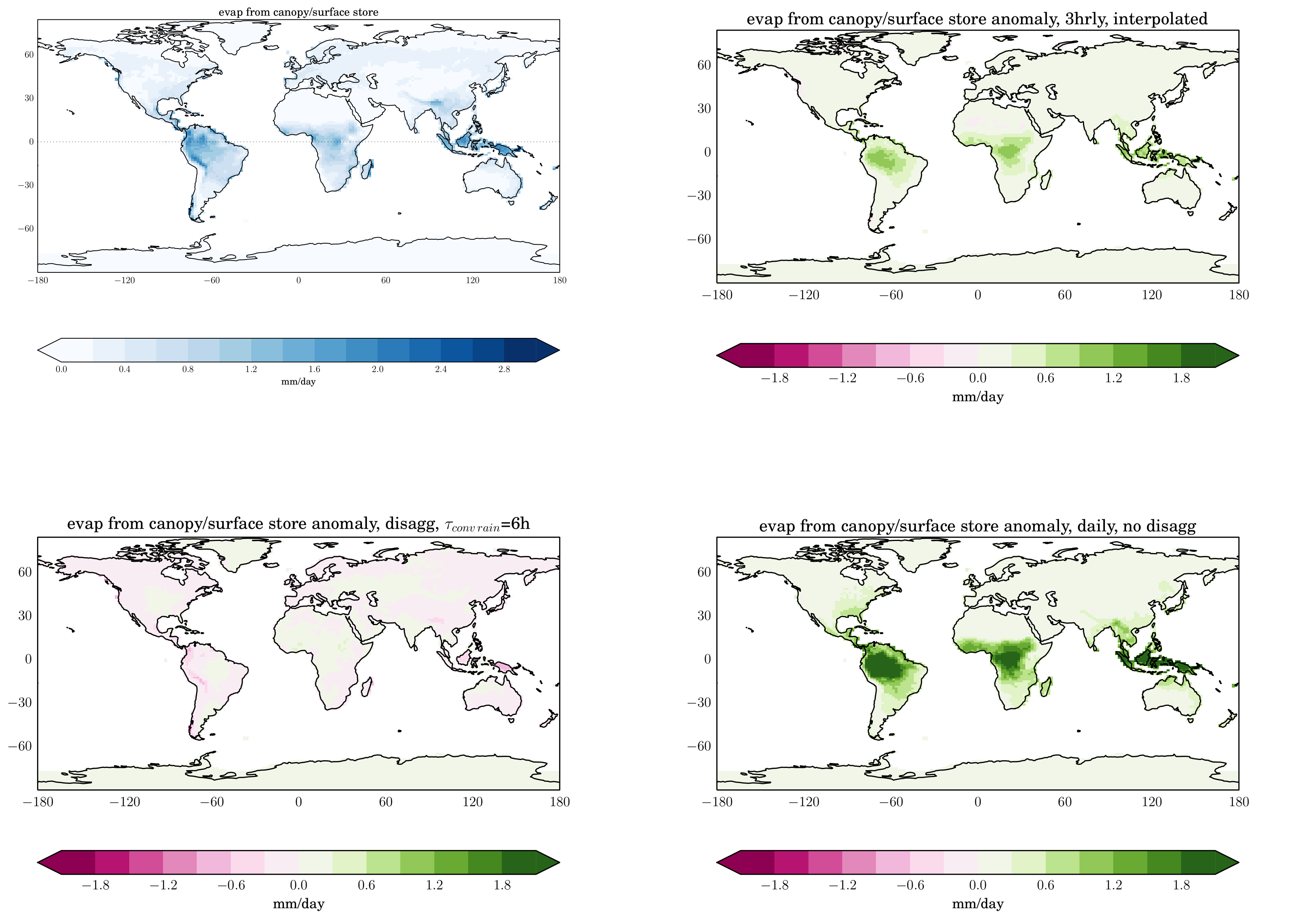

Figure 8: Top left: Output variable from JULES run with full 20 minute resolution forcing. Top right: Anomalies with respect to the full result, using 3 hourly forcing with interpolation. Bottom left: Anomalies with respect to the full result, using disaggregation with default event durations. Bottom right: Anomalies with respect to the full result, using daily forcing with no interpolation.

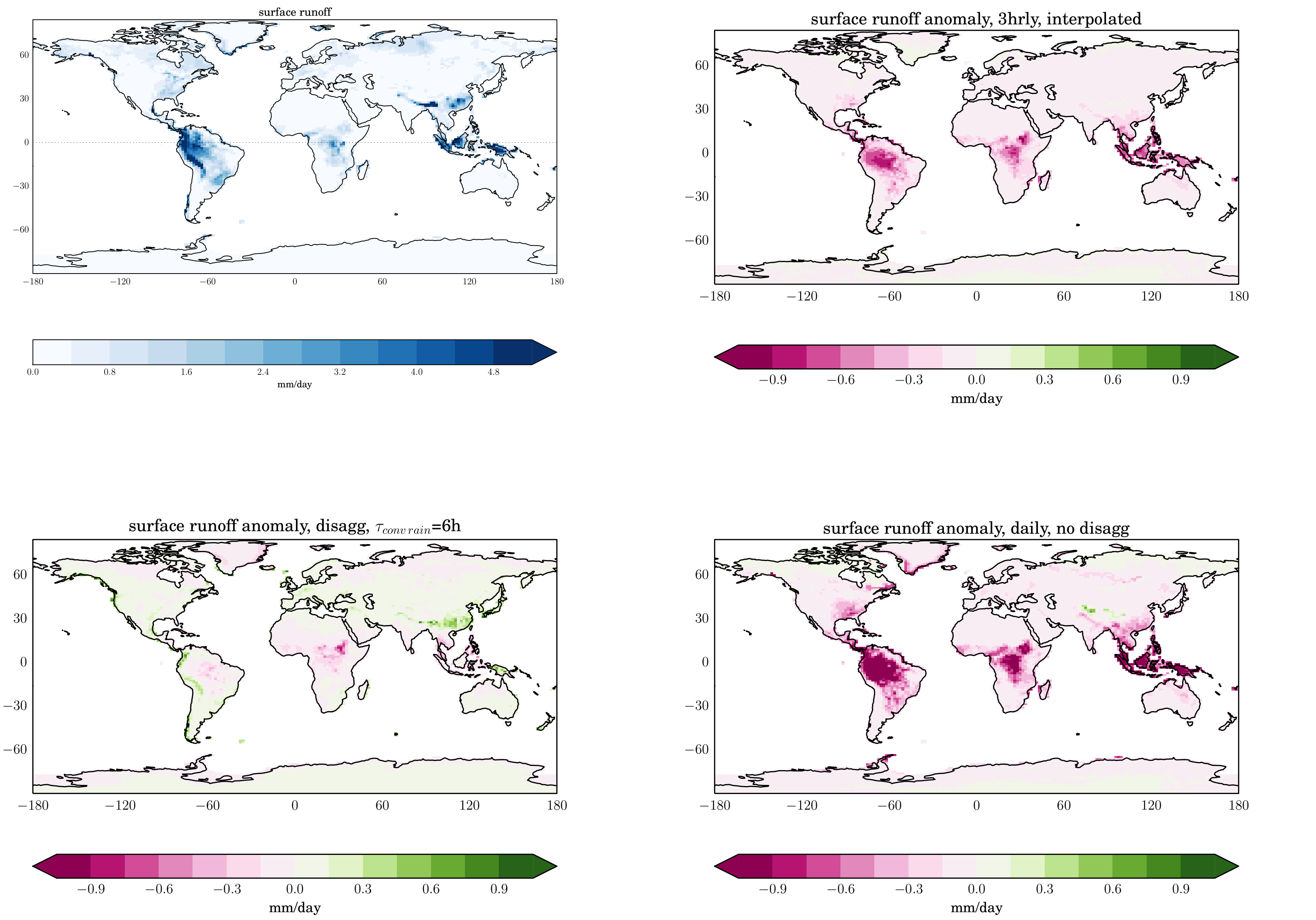

Figure 9: Top left: Output variable from JULES run with full 20 minute resolution forcing. Top right: Anomalies with respect to the full result, using 3 hourly forcing with interpolation. Bottom left: Anomalies with respect to the full result, using disaggregation with default event durations. Bottom right: Anomalies with respect to the full result, using daily forcing with no interpolation.

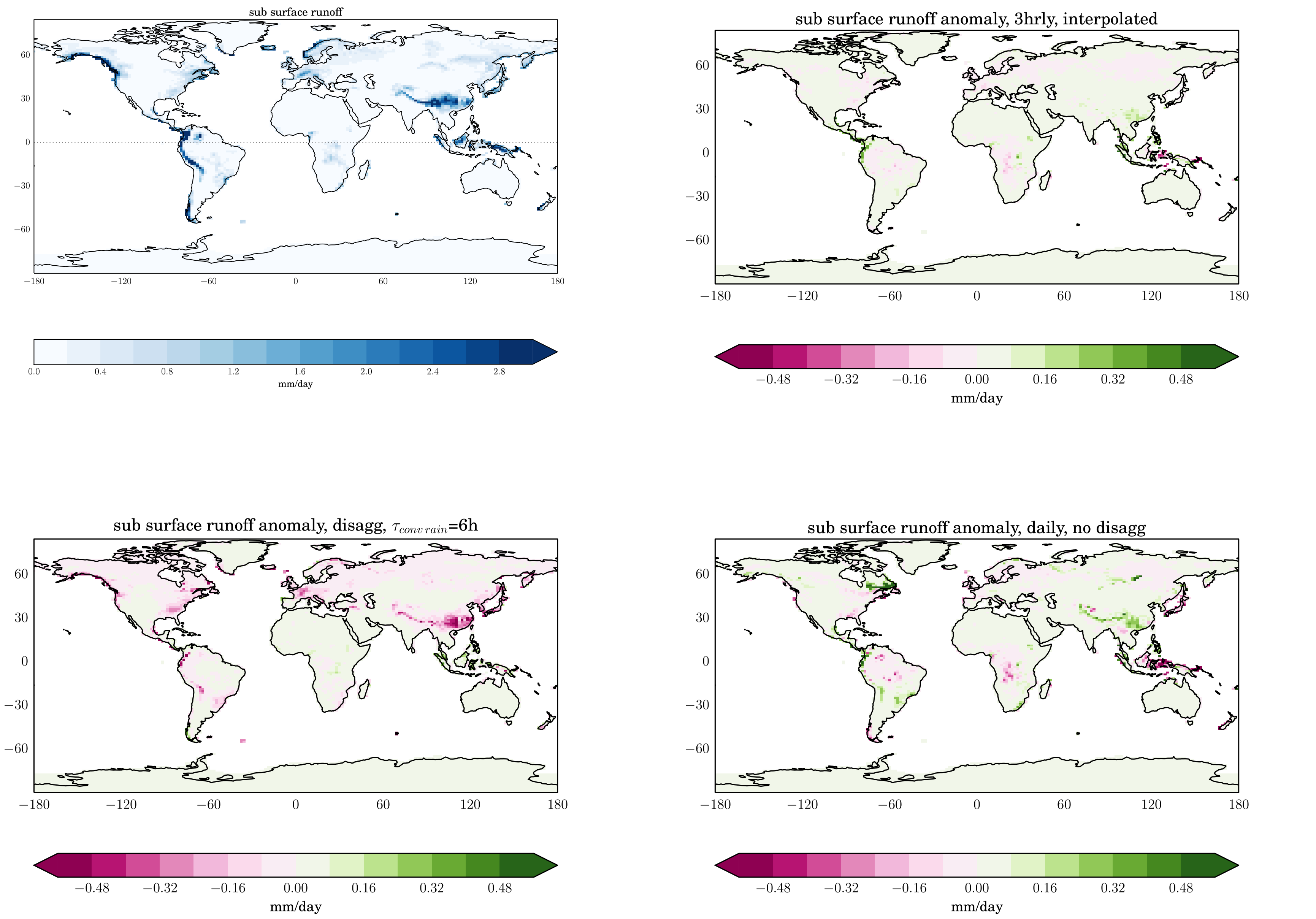

Figure 10: Top left: Output variable from JULES run with full 20 minute resolution forcing. Top right: Anomalies with respect to the full result, using 3 hourly forcing with interpolation. Bottom left: Anomalies with respect to the full result, using disaggregation with default event durations. Bottom right: Anomalies with respect to the full result, using daily forcing with no interpolation.

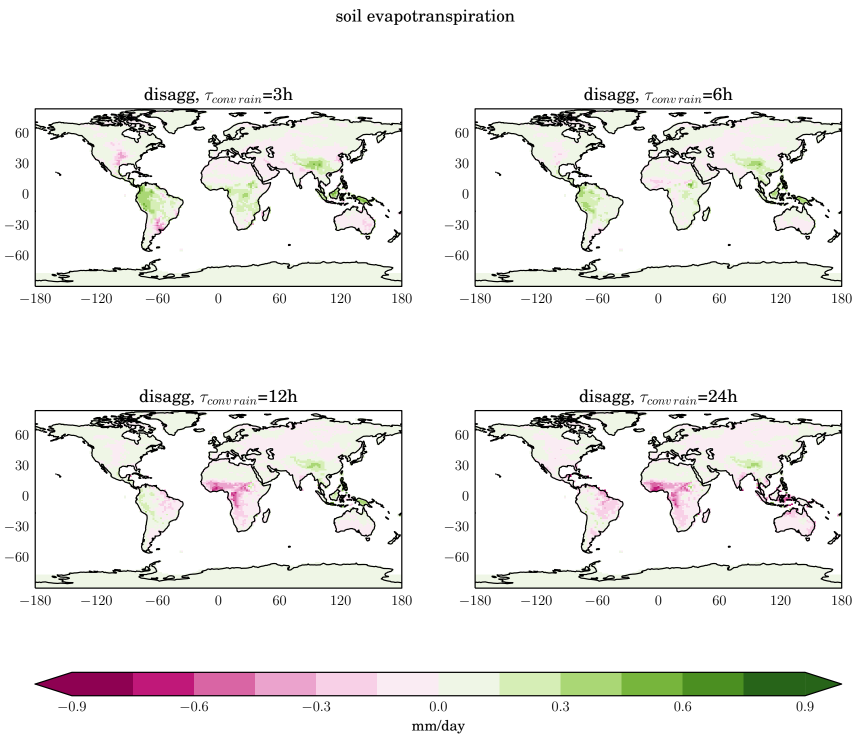

Figure 11: Anomalies with respect to the full result, using disaggregation with convective rain event durations of 3 hours (top left), 6 hours (top right), 12 hours (bottom left) and 24 hours (bottom right).

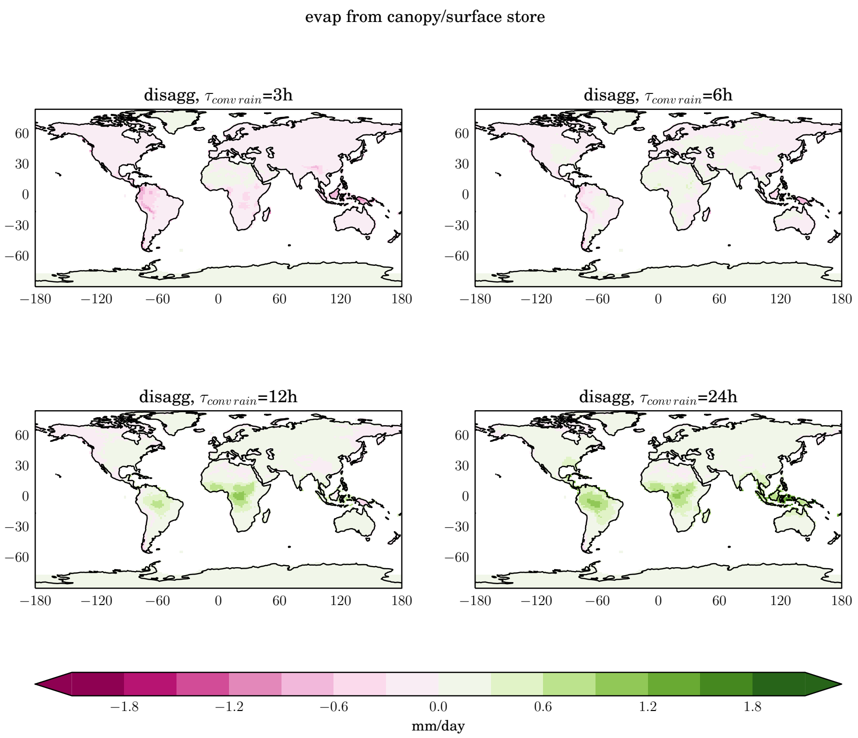

Figure 12: Anomalies with respect to the full result, using disaggregation with convective rain event durations of 3 hours (top left), 6 hours (top right), 12 hours (bottom left) and 24 hours (bottom right).

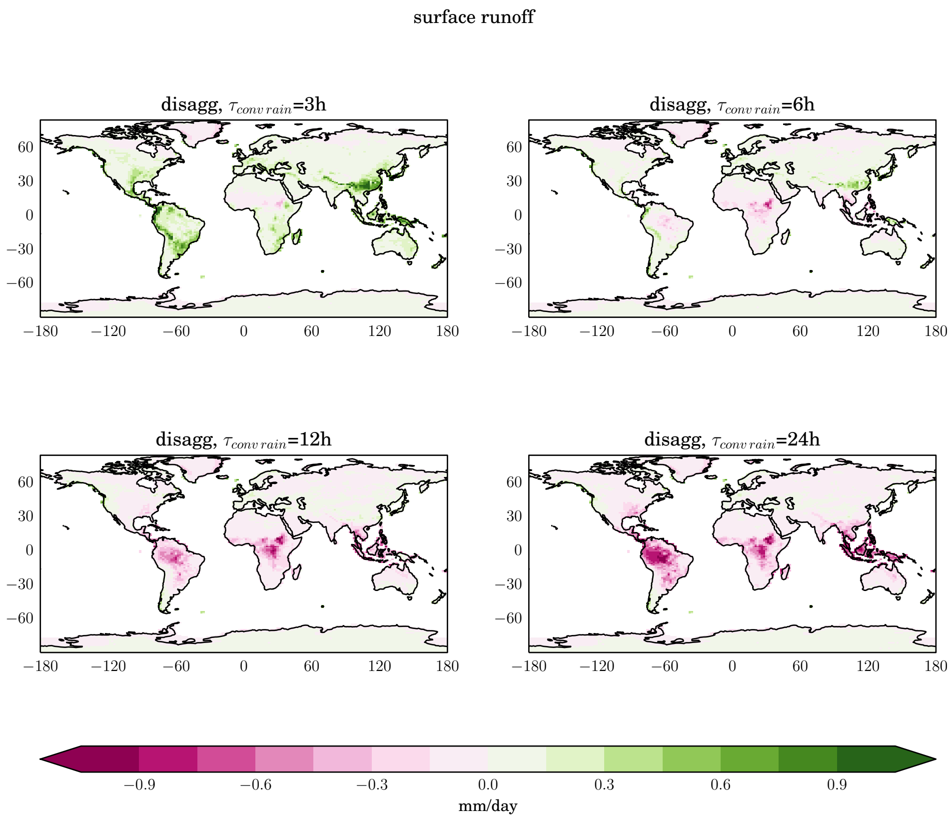

Figure 13: Anomalies with respect to the full result, using disaggregation with convective rain event durations of 3 hours (top left), 6 hours (top right), 12 hours (bottom left) and 24 hours (bottom right).

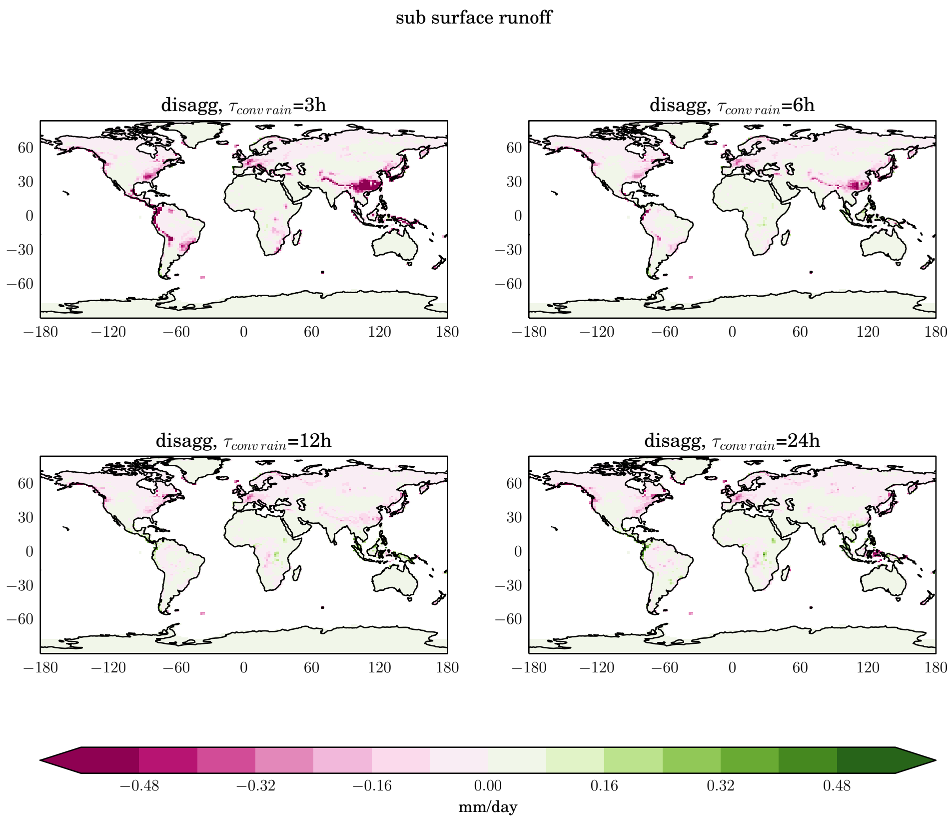

Figure 14: Anomalies with respect to the full result, using disaggregation with convective rain event durations of 3 hours (top left), 6 hours (top right), 12 hours (bottom left) and 24 hours (bottom right).

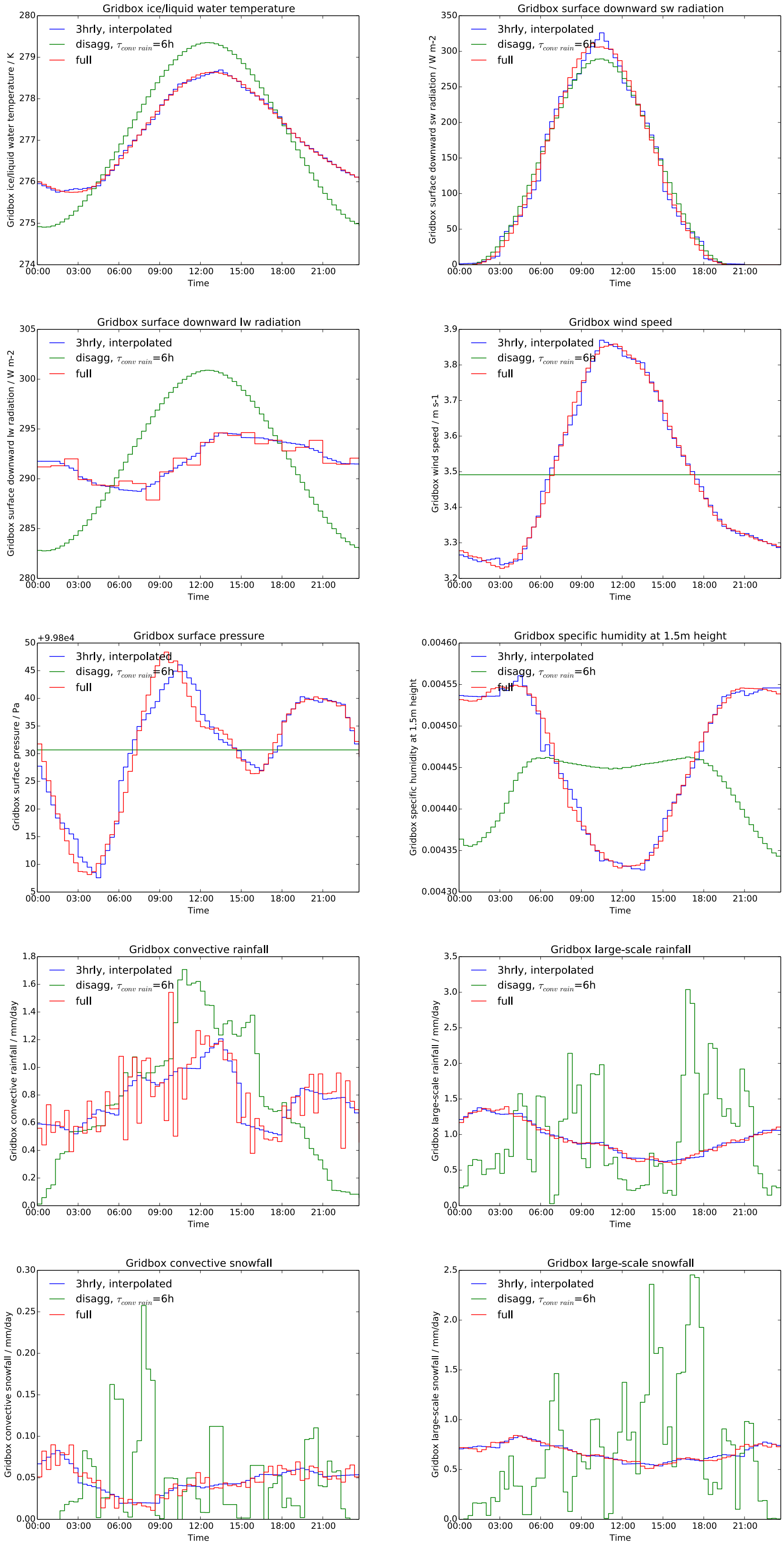

Figure 15: Diurnal cycle of driving data for the Hyytiala FLUXNET site, Finland, averaged over the days in 1984.

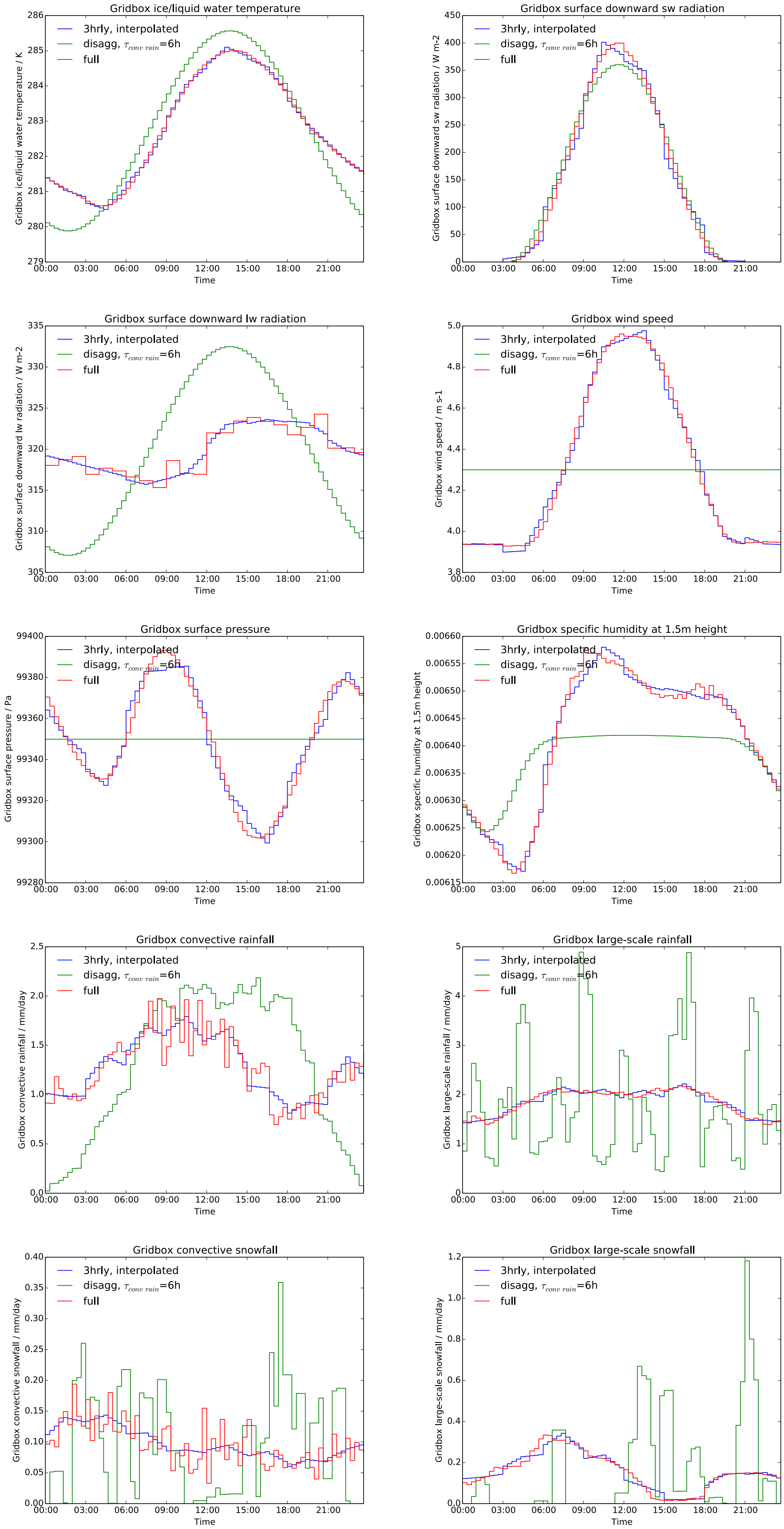

Figure 16: Diurnal cycle of driving data for the Vielsalm FLUXNET site, Belgium, averaged over the days in 1984.

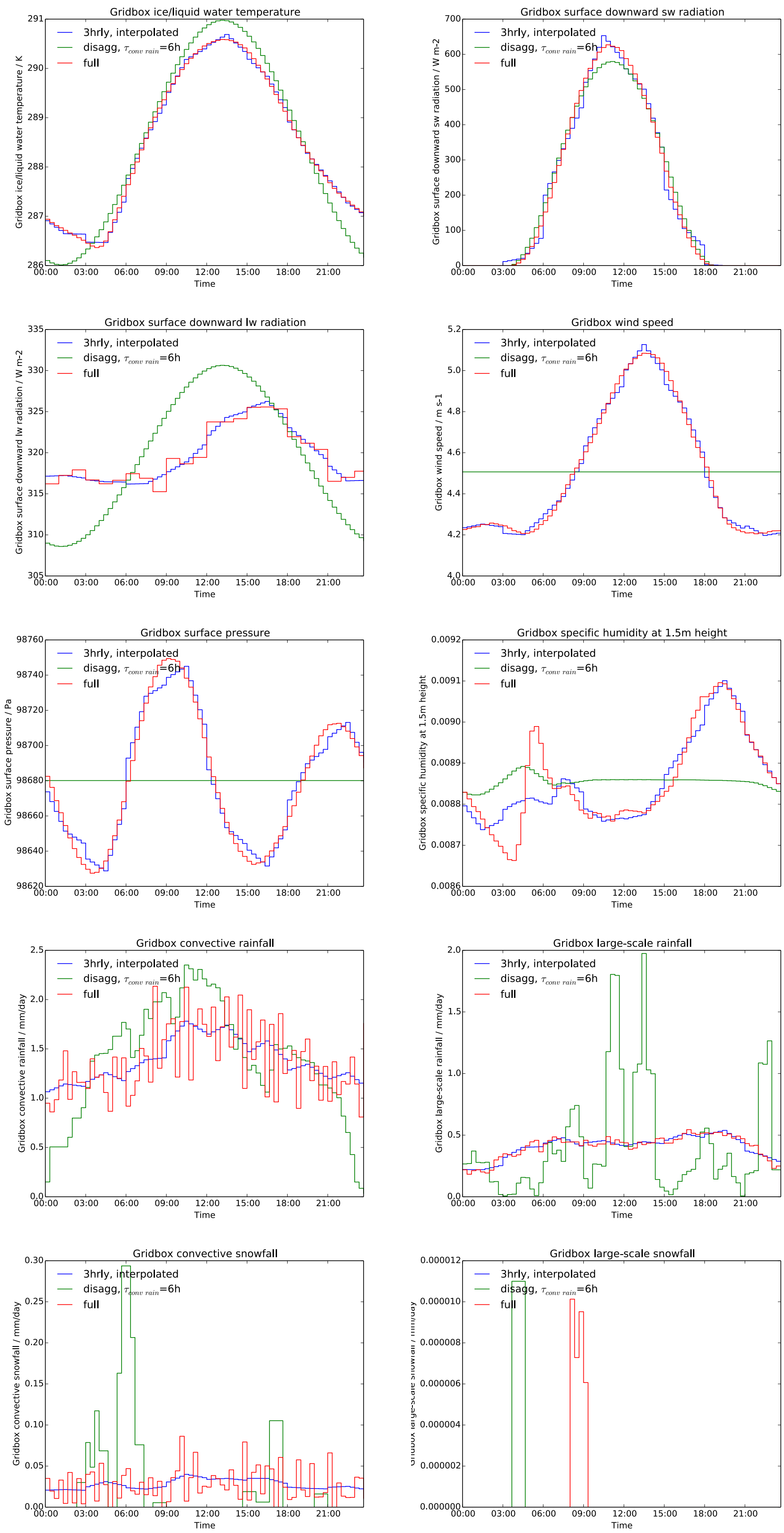

Figure 17: Diurnal cycle of driving data for the Collelongo FLUXNET site, Italy, averaged over the days in 1984.

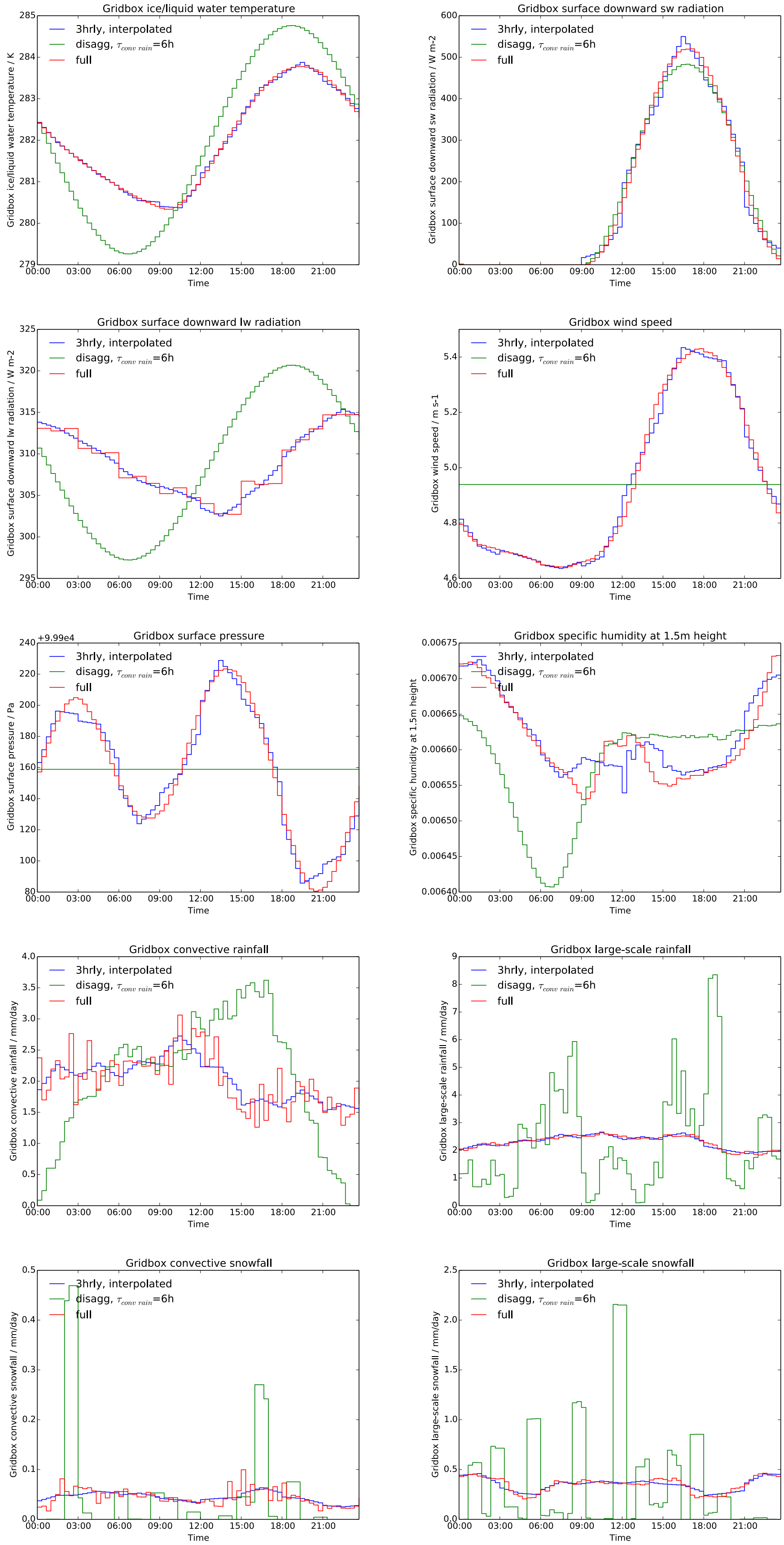

Figure 18: Diurnal cycle of driving data for the Harvard Forest FLUXNET site, Massachusetts, averaged over the days in 1984.

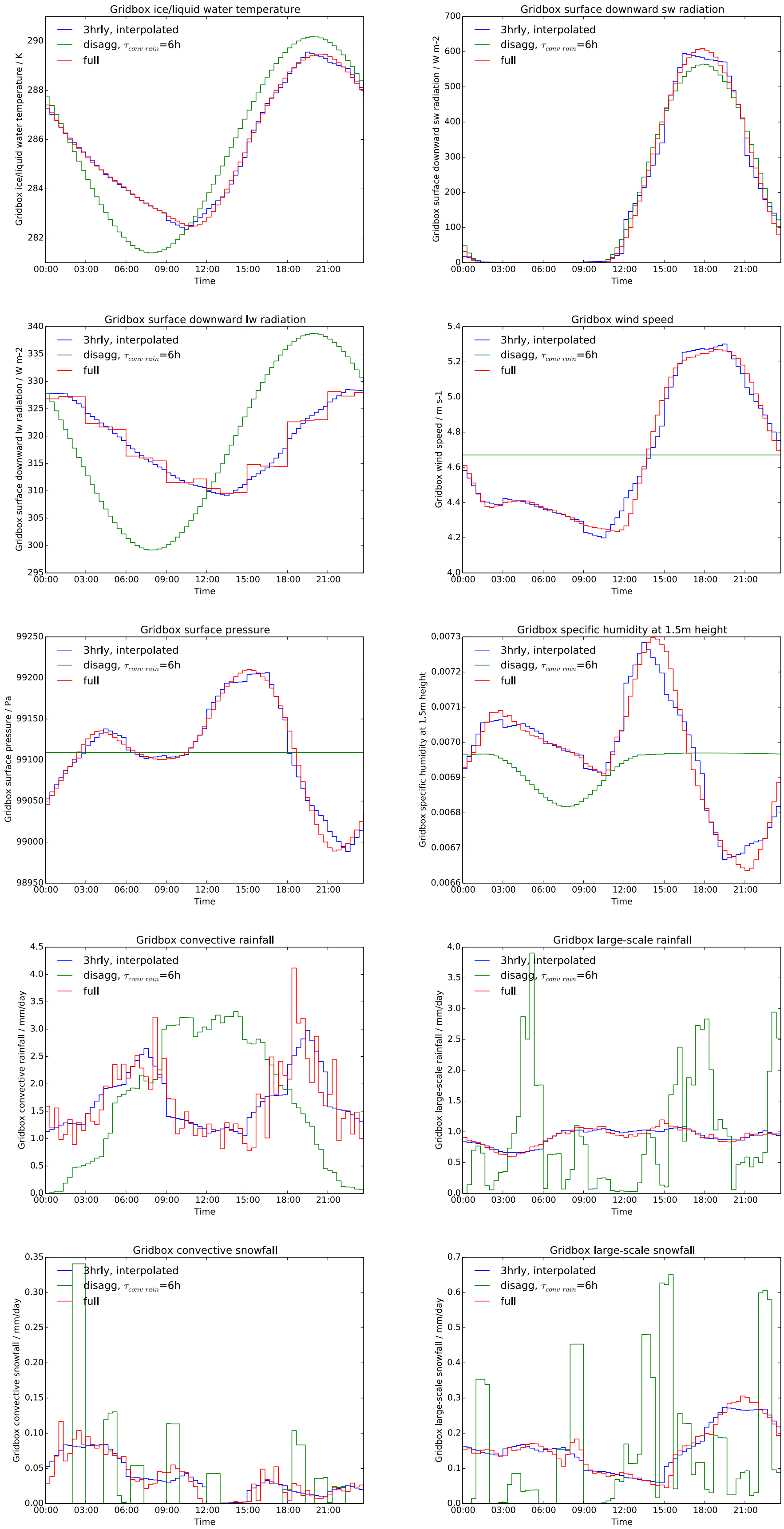

Figure 19: Diurnal cycle of driving data for the Bondville FLUXNET site, Illinois, averaged over the days in 1984.

Met Office
FitzRoy Road, Exeter
Devon, EX1 3PB
UK

Tel: 0870 900 0100
Fax: 0870 900 5050
enquiries@metoffice.gov.uk
www.metoffice.gov.uk